Hindawi
International Journal of Photoenergy
Volume 2022, Article ID 2133294, 21 pages
https://doi.org/10.1155/2022/2133294

Research Article

An Advanced MPPT Scheme for PV Systems Application with Less Output Ripple Magnitude of the Boost Converter

Abdelkhalek Chellakhi,[1] **Said El Beid**,[2] **and Younes Abouelmahjoub**[1]

[1]*LabSIPE at National School of Applied Sciences, Chouaib Doukkali University, El Jadida 2400, Morocco*
[2]*CISIEV Team, Cadi Ayyad University, Marrakech 40160, Morocco*

Correspondence should be addressed to Abdelkhalek Chellakhi; chellakhi.a@ucd.ac.ma

Received 15 February 2022; Revised 16 August 2022; Accepted 2 September 2022; Published 24 September 2022

Academic Editor: Leonardo Sandrolini

The purpose of this paper is to enhance the performance and tracking efficiency of solar photovoltaic systems. This aim can be achieved by operating the photovoltaic array at its optimum power and reducing the output ripple problem of DC-DC converters that affect and stress sensible electronic loads. In view of that, an advanced maximum power point (MPP) tracking (MPPT) scheme, which can guarantee zero oscillation tracking of the accessible MPP and less ripple magnitude on the output side of the DC-DC boost converter, is used. Various simulations are carried out under three conditions of solar irradiance variation, namely, standard test conditions (STC), rapid, and Sin scenarios, using the MATLAB/Simulink® environment, to assess and benchmark the robustness of the tracking of the new MPPT scheme over the celebrated Increment of Conductance (INC) MPPT scheme. Based on the simulation results, the proposed scheme can significantly improve tracking accuracy and reduce the magnitude of ripples on both sides of the boost converter compared to the INC scheme. Certainly, the proposed scheme can provide a shorter time response (0.011 seconds) to locate and track the expected MPP, which is 2.55 times less than that of the INC scheme; a zero power magnitude oscillation instead of 15.9 watts of the INC scheme; and six-time minimization of the magnitude of output voltage ripples compared to the INC scheme. Furthermore, the suggested MPPT scheme has the better tracking efficiency in all scenarios; 99.86%, 99.60%, and 99.62% in the STC, rapid, and Sin scenarios, respectively, with an average value of 99.69% compared to the INC MPPT scheme, which has 94.23%, 95.28%, and 97.87% in the STC, rapid, and Sin scenarios, respectively, with a moderate average tracking efficiency of 95.79%. Finally, the accuracy and tracking performance of the proposed MPPT scheme are verified by real-time examination using the RT-LAB simulator. According to the results obtained, the proposed scheme provides the highest tracking efficiency of 99.80% and 97.77% under the STC and sudden insolation change scenarios, respectively, compared to the INC scheme, which shows, respectively, 97.8% and 96.5% under both scenarios.

1. Introduction

Due to their sustainability and cleanness, renewable energies have multiple benefits for the environment and economic sectors. According to the analysis of the International Renewable Energy Agency (IRENA), renewable energy is becoming an essential pathway for deployment, besides the decrease in energy related to CO_2 emissions can reach more than 90% [1, 2]. Without a doubt, and in fewer years, renewable energy resources will be the ground zero of electrical energy generation. Indeed, this can be reasonable in view of the tremendous research and applications that have been conducted in this field, in addition to the accelerated development in the smart technologies used. In this context, solar photovoltaic energy is considered the most attractive and interesting among other renewable energy resources because of its cleanliness, ease of implementation, and low cost. However, the effectiveness of the photovoltaic system is greatly dependent on two climatic conditions: solar irradiation and ambient temperature [3]. Moreover, because of the nonlinearity of the power versus voltage (P-V) characteristics of the photovoltaic module, a single optimal power

point (MPP) can appear in the P-V curves. To follow and extract this MPP, a specific tracking mechanism called maximum power point tracking (MPPT) is required [3].

The scientific literature contains many MPPT schemes for applications in the photovoltaic system [4–6]. From these MPPT algorithms, it can distinguish between three categories: direct, indirect, and intelligent MPPT techniques [7]. Direct MPPT schemes, such as perturbation and observation (P&O) [8], increment of conductance (INC) [3, 9], and hill climbing (HC) [10], are widely used due to their simplicity, ease of implementation, and photovoltaic panel independence. However, these techniques have serious problems that reduce their tracking performance. For that reason, many improved versions of algorithms based on the aforementioned traditional direct methods are suggested [11–16] including indirect MPPT schemes, such as fractional open-circuit voltage (FOCV) [17] and short-circuit current (FSCC) [18]; intelligent techniques MPPT schemes include fuzzy logic controller (FLC) [19, 20], partial swarm optimization (PSO) [21, 22], firefly algorithm (FA) [23], ant colony optimization (ACO) [24], neural network algorithm (NNA) [24], hybrid adaptive neurofuzzy inference system flower pollination algorithm (ANFIS-FPA) [25], and hybrid adaptive neurofuzzy inference system (ANFIS) and artificial bee colony (ABC) algorithm [26]. These MPPT schemes differ in some factors, such as fluctuations in steady-state operation, convergence speed, especially under fast irradiation or temperature change, complexity, required sensors, time response, and tracking of the real MPP at partial shading effect [2]. The latter dramatically affects the P-V curves of the photovoltaic array, which exhibits at least two MPPs. The first, which has a lower level of power, is called the local MPP (LMPP), while the other is named the global MPP (GMPP), at which the maximum power can be reached. In this sense, tracking MPP under partial shading conditions (PSC) is a complex task for traditional schemes such as P&O, INC, and HC, which generally do not track GMPP [27]. For this reason, improved techniques are proposed to track MPP under PSC [28–32].

However, fluctuations around the MPP at steady-state operation, convergence speed, and time response remain the main drawbacks affecting MPPT efficiency. Moreover, many conventional MPPT schemes complain of another drawback, which is rarely discussed in the literature review, such as high ripple magnitude and nonstability in the output of DC-DC converters, as reported by Abdelkhalek et al. [2]. The existence of a high ripple magnitude in the output of the DC-DC converter can significantly affect the performance of the system and destroy sensible DC loads, which need a stable input from the converter.

In this regard, and to address the aforementioned shortcomings, an advanced MPPT scheme published recently by Chellakhi et al. [8] is used. This latter can provide a good compromise between MPP tracking and fewer output ripple magnitudes of the boost converter compared to conventional MPPT schemes such as INC MPPT, as reported in a previously published paper [2].

This paper is an extension of the work originally presented at the 2020 International Conference on Electronics, Control, Optimization, and Computer Science (ICECOCS'20) [2].

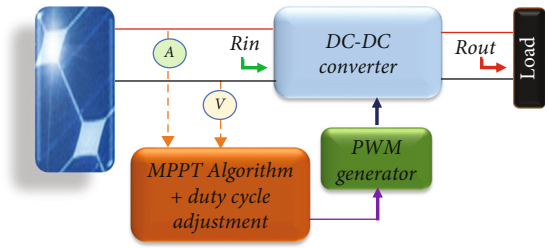

Figure 1: Schematic diagram of the complete photovoltaic system used.

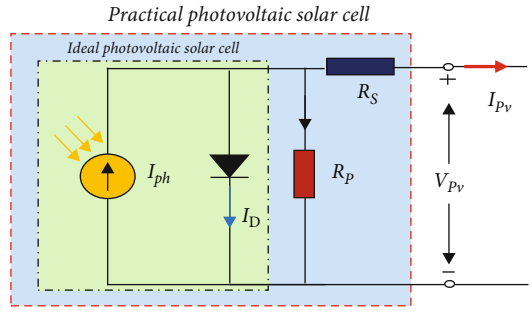

Figure 2: Photovoltaic solar cell equivalent circuit.

Hence, this work presents the following contributions and novelties:

(i) More simulation cases with detailed comparison results are added to investigate the performance of the proposed MPPT strategy according to the MPP tracking accuracy and ripple magnitude mitigation in the output of the DC-DC boost converter

(ii) A detailed and comprehensive numerical simulation analyses of ripple problem using a new proposed MPPT scheme and the INC MPPT technique

(iii) A real-time verification based on the RT-LAB simulator environment is also carried out to evaluate the capability and performance of the suggested MPPT scheme in real-time implementation

This paper is organized as follows: Section 2 shows the analysis of the components of the photovoltaic system. Section 3 explains the principles of the proposed MPPT and INC MPPT schemes. Next, the simulation and discussion are presented in Section 4, while the real-time verification using the RT-LAB simulator environment is described in Section 5. Finally, the conclusion of this study is reported in Section 6.

2. Analysis of Photovoltaic System Components

The overall photovoltaic system used in this study is depicted in Figure 1, where five essential components are

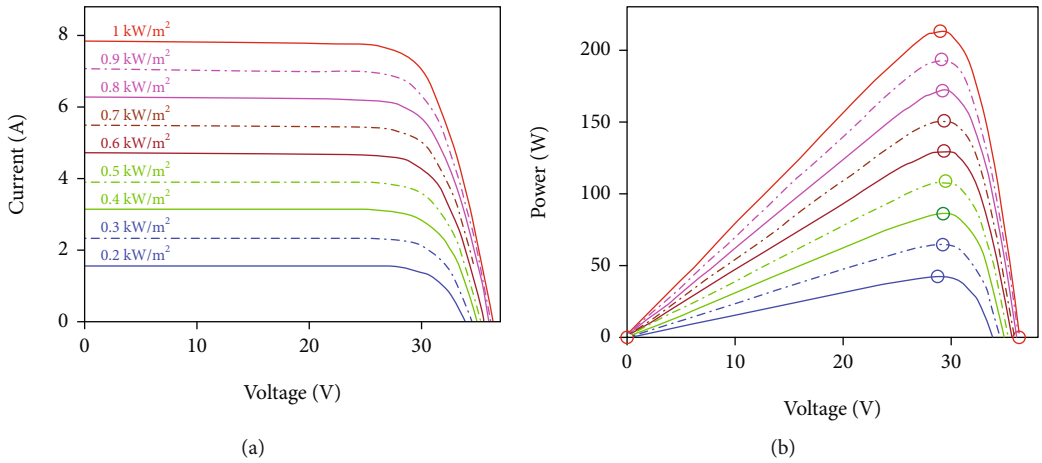

Figure 3: Characteristics of the photovoltaic module used (a) I-V and (b) P-V under $G = 1\,\text{kW/m}^2$ and $T = 25^\circ\text{C}$.

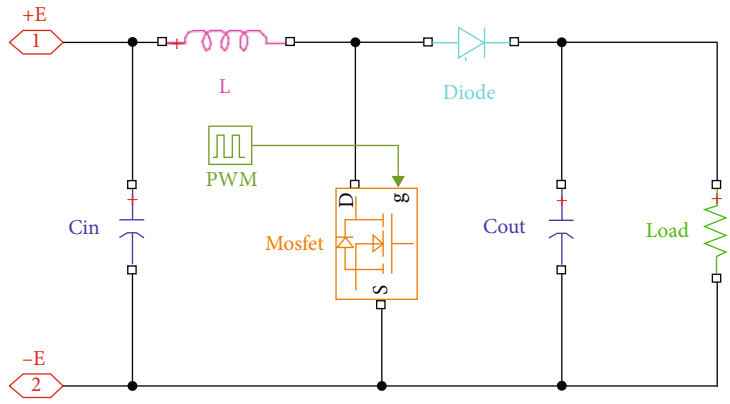

Figure 4: Simulink implementation circuit of the DC-DC boost converter with resistive load.

depicted: photovoltaic generator, DC-DC converter, MPPT controller, PWM generator, and load. In this section, two subsections are reported. The equivalent circuit model and characteristics of the photovoltaic cell will be described in the first section, while a brief overview of the DC-DC boost converter will be found in the second section.

2.1. Photovoltaic Cell Model. The photovoltaic module contains numerous units of solar cells, also called photovoltaic cells, placed in parallel and/or series to obtain the desired photovoltaic module with the required current and voltage. Due to the insufficient power of a single photovoltaic module, this latter will be joined with other photovoltaic modules to form a photovoltaic array system.

Figure 2 illustrates the equivalent circuit of a photovoltaic cell, which contains two resistances and a diode. The R_S series resistance signifies the losses of the metal grid, contacts, and the current collecting bus, where the R_P parallel resistance characterizes the flow of small leakage current through the parallel path losses [2, 8].

From the equivalent circuit of the photovoltaic cell presented in Figure 2, the mathematical expression of the pho-

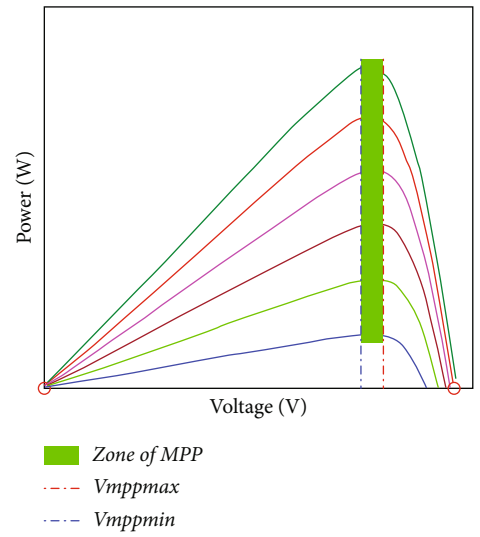

Figure 5: Illustration of the MPP zone in P-V curves under different insolation levels [8].

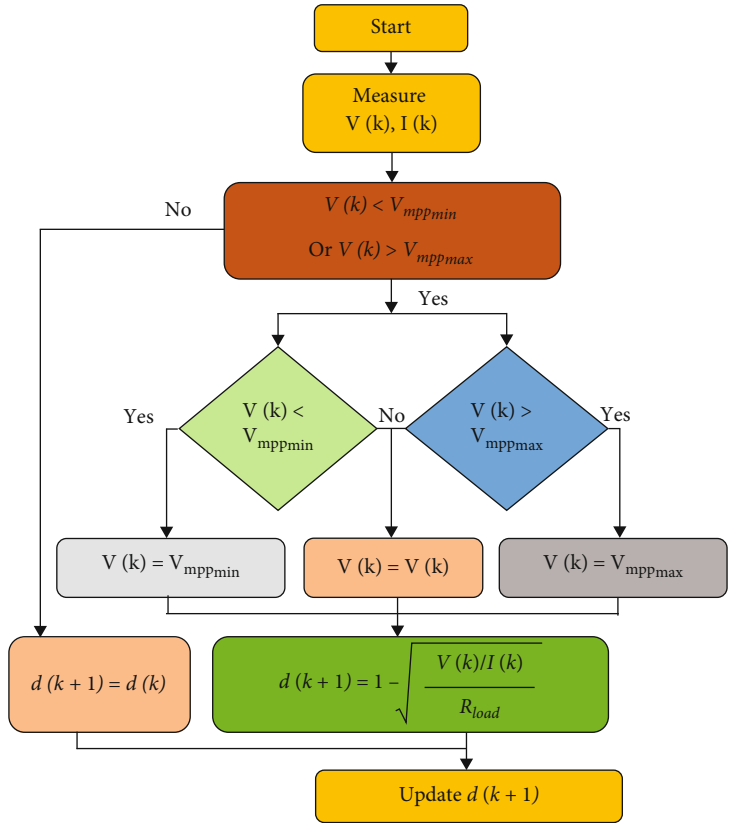

Figure 6: Flowchart of the suggested MPPT scheme.

tovoltaic cell output current I_{pv} can be given as follows [33–35]:

$$I_{pv(cell)} = I_{ph} - I_s\left(exp\left(\frac{V_{pv} + I_{pv} \times R_S}{V_t}\right) - 1\right) - \frac{\left(V_{pv} + I_{pv} \times R_S\right)}{R_P}. \quad (1)$$

Basically, a photovoltaic panel module is made by linking several solar photovoltaic cells in parallel (Np) and in series (Ns). Thus, and according to Equation (1), the mathematical expression of the output current of the photovoltaic module can be written as follows [33–35]:

$$I_{pv(\text{module})} = N_p \times I_{ph} - N_p \times I_s\left[exp\left(\frac{V_{pv} + I_{pv} \times R_S}{N_s \times V_t}\right) - 1\right] - N_p \times \frac{V_{pv} + I_{pv} \times R_S}{N_s \times R_P}, \quad (2)$$

$$V_t = \frac{A \times K \times T}{q},$$

where V_t is the thermal voltage of the photovoltaic cell.

When a photovoltaic module is exposed to different variations of environmental conditions, especially to different sun irradiations, its output P-V and I-V characteristics show noticeable affectations, as reported in Figure 3.

2.2. DC-DC Boost Converter. The maximum power point (MPP) of the photovoltaic module can be far from the operating point (OP) when the photovoltaic module is directly connected to a DC load. This OP will be the intersection of the I-V curve of the photovoltaic module with the DC load line [36]. For this purpose and to enhance the accuracy of the photovoltaic system, DC-DC converters are usually used between the photovoltaic module and load. Due to its simplicity and high reliability regarding other more complex configurations, the DC-DC Boost converter is the most used among several converters. It guarantees a better transfer of energy between the photovoltaic module and the load by matching the OP with the MPP of the photovoltaic module. Figure 4 depicts the circuit of the DC-DC boost converter connected to a load [2, 8].

The relationships between the input and output sides of the boost converter in the case of current and voltage with the duty ratio are given as follows:

$$V_{\text{out}} = V_{pv}\frac{1}{1-d}, \quad (3)$$

$$I_{\text{out}} = I_{pv}(1-d). \quad (4)$$

By division of Equation (3) by Equation (4), it results in Equation (5).

$$R_{\text{out}} = R_{\text{load}} = \frac{V_{\text{out}}}{I_{\text{out}}} = \frac{1}{(1-d)^2} \times \frac{V_{pv}}{I_{pv}}, \quad (5)$$

where R_{load} is the charge resistance.

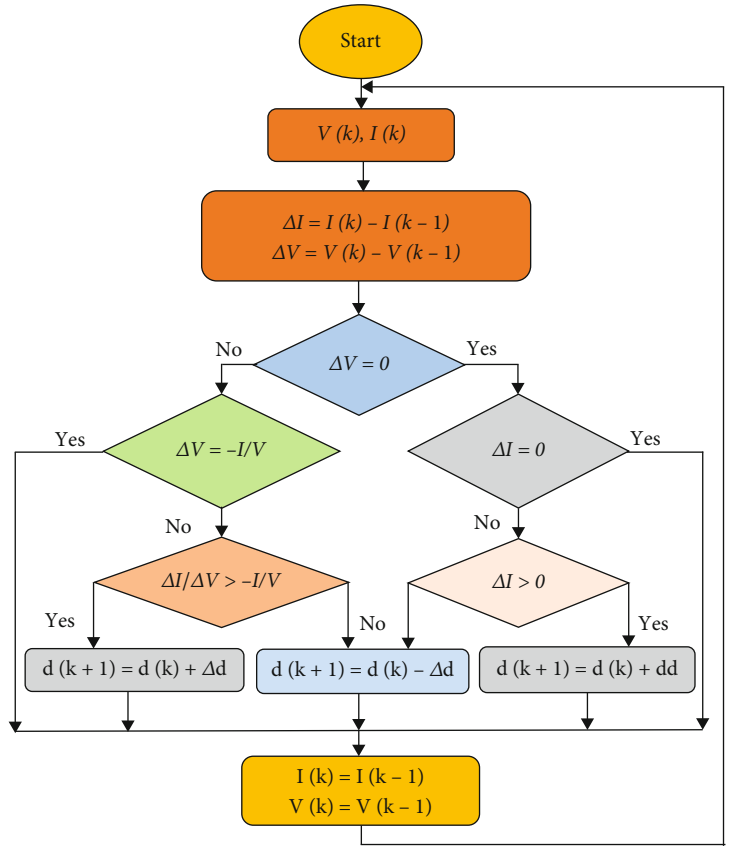

Figure 7: Flowchart of the INC MPPT scheme.

Table 1: Parameters of the 1soltech 1sth-215-p photovoltaic module at STC, DC-DC boost converter, and load.

Parameters	Value
Photovoltaic module	
Maximum power (*P*mpp)	213.15 W
Voltage at MPP (*V*mpp)	29 V
Current at MPP (*I*mpp)	7.35 A
Open circuit voltage (*V*oc)	36.3 V
Short circuit current (*I*sc)	7.84 A
Temperature coefficient of Voc	-0.36099 (%/°C)
Temperature coefficient of Isc	0.102 (%/°C)
DC-DC converter	
Input capacitor	47 μF
Output capacitor	470 μF
Inductance	1 mH
Switching frequency	10 KHz
Load	
Resistive load	30 Ω

In the basis of Equation (5), the DC-DC boost converter duty ratio can be given as follows:

$$d = 1 - \sqrt{\frac{V(k)/I(k)}{R_{\text{Load}}}}. \tag{6}$$

3. Proposed MPPT and INC MPPT Scheme Principles

3.1. Proposed MPPT Scheme Principle. The principle of the suggested MPPT scheme is detailed in the previous work of Chellakhi et al. [8]. As illustrated in Figure 5, the essential idea of the suggested scheme is based on the P-V characteristics at different levels of insolation with a fixed ambient temperature level, where it should be noted that the interval of the MPPs (zone of MPPs) is very narrow and it is limited by two values of voltage, $V\text{mpp}_{\text{min}}$ and $V\text{mpp}_{\text{max}}$ [8].

The block diagram of the suggested MPPT scheme is presented in Figure 6, where it can be seen that the suggested MPPT scheme has a direct control strategy to track the expected MPP. By far, after the measurement and voltage regulation stages, Equation (7) is used to directly calculate

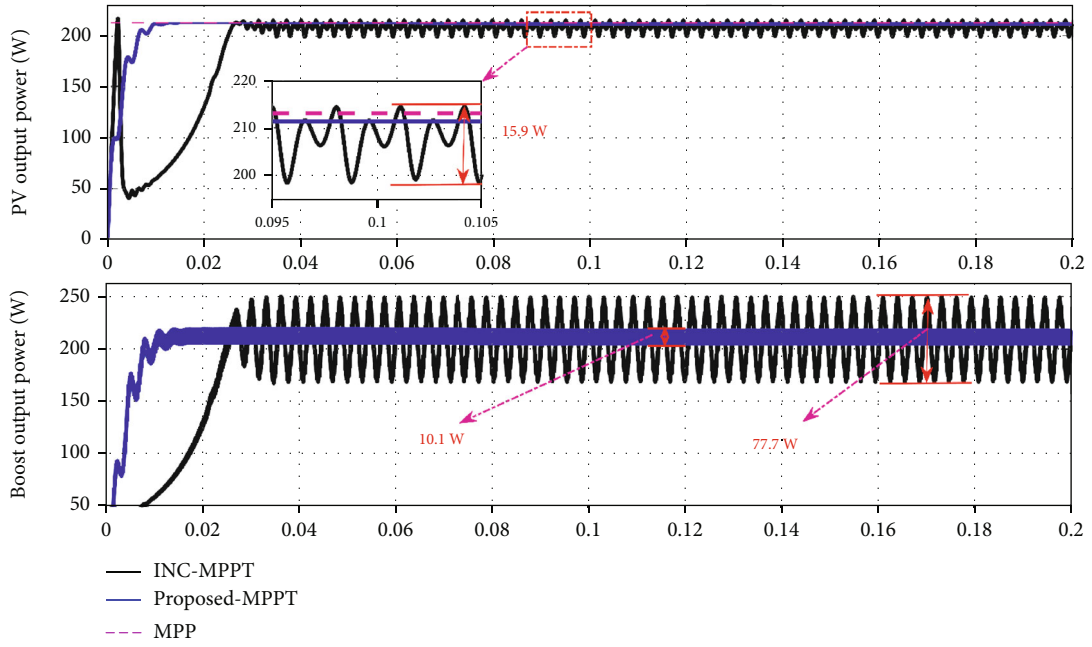

Figure 8: Simulation result curves of the output power of the photovoltaic module and the boost converter under STC.

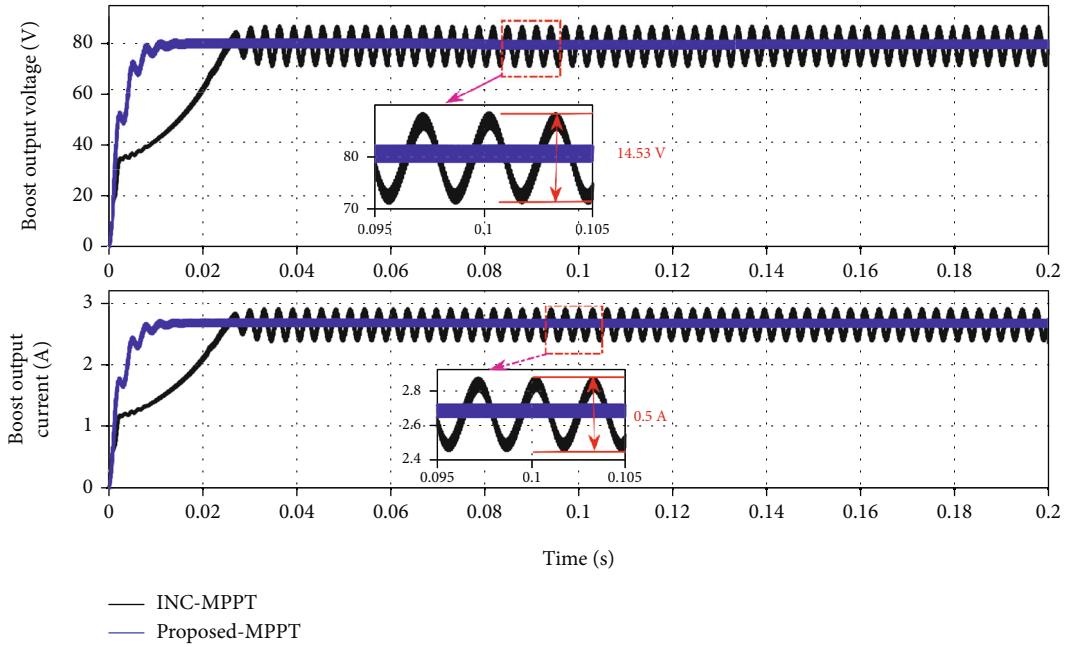

Figure 9: Simulation results of the output current and voltage of the boost converter under STC.

the new duty ratio by substituting the sensed current, the regulated voltage, and the load charge value.

$$d(k+1) = 1 - \sqrt{\frac{V(k)/I(k)}{R_{\text{Load}}}}. \tag{7}$$

3.2. INC MPPT Scheme Principle. The increment of conductance (INC) scheme has been used in many works [3, 37] to deal with the disadvantages of the conventional P&O MPPT scheme, the steady-state fluctuation around the MPP and the loss of tracking under an abrupt change in solar irradiation. The INC MPPT scheme employs the slope of the power versus voltage (P-V) curves to track the expected MPP. Its principle is related to the derivative of dP/dV of the power curve of the PV module or array, which is equal to zero at the MPP, less than zero when the MPP stays on the right side, and greater than zero when

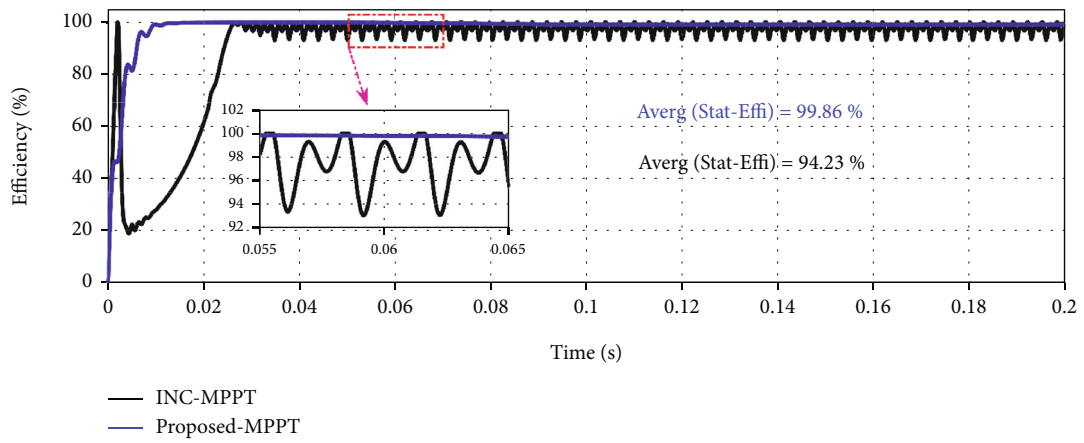

Figure 10: Simulation results of tracking efficiency under STC.

Table 2: Comparison of the STC simulation results of the proposed MPPT and INC MPPT schemes.

	INC MPPT	Proposed MPPT
Photovoltaic module output		
Power ripple magnitude (W)	15.9	Neglected
SSE (W)	6.55	1.6
Boost converter output		
Power ripple magnitude (W)	76	10
Voltage ripple magnitude (V)	15	2.5
Current ripple magnitude (A)	0.5	0.1
Time response (s)	0.028	0.011
Steady-state average efficiency (%)	94.23	99.86

the MPP stays on the left side [3]. The latter can be mathematically expressed as

$$\frac{dP}{dV} = I + V\frac{dI}{dV} = 0,$$

$$\frac{dI}{dV} \cong \frac{\Delta I}{\Delta V} = -\frac{I_{\mathrm{MPP}}}{V_{\mathrm{MPP}}},$$

$$\begin{cases} \dfrac{\Delta I}{\Delta V} = -\dfrac{I}{V} & \text{At MPP,} \\ \dfrac{\Delta I}{\Delta V} > -\dfrac{I}{V} & \text{Left of MPP} \\ \dfrac{\Delta I}{\Delta V} < -\dfrac{I}{V} & \text{Right of MPP.} \end{cases} , \quad (8)$$

Based on the comparison of the instantaneous conductance (I/V) value with the incremental conductance ($\Delta I/\Delta V$) value, the MPP can be followed as described in the block diagram of the INC MPPT scheme depicted in Figure 7.

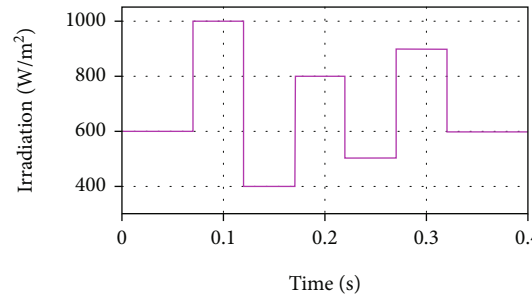

Figure 11: Rapid variation of solar irradiation profile.

4. Simulation and Results

To illustrate the effectiveness of the suggested MPPT scheme, a comparison with the INC MPPT scheme is carried out under different atmospheric conditions. The first scenario was the STC conditions, then a rapid insolation change was adopted as the second test, and the final scenario was a Sin test, which is a slow solar irradiation change. It is noteworthy to mention that the ambient temperature was considered fixed at 25°C. MATLAB/Simulink® software (R2018a) was used in the numerical implementation. The 1Soltech 1STH-215-P photovoltaic module and the DC-DC boost converter with load specifications are listed in Table 1.

4.1. Standard Test Conditions (STC). The simulation results of the suggested MPPT scheme compared with the INC MPPT scheme are presented in Figures 8 and 9. These figures illustrate the output power of the photovoltaic module and the output power, voltage, and current of the boost converter.

Based on the simulation results described in Figure 8, it is clear that the INC MPPT scheme has a long tracking time (0.026 seconds) to track the MPP, and it shows noticeable steady-state ripples in the output power of the photovoltaic module and boost converter, leading to high power losses. On the contrary, the suggested MPPT scheme can track the real MPP with a fast tracking time (0.012 seconds) and

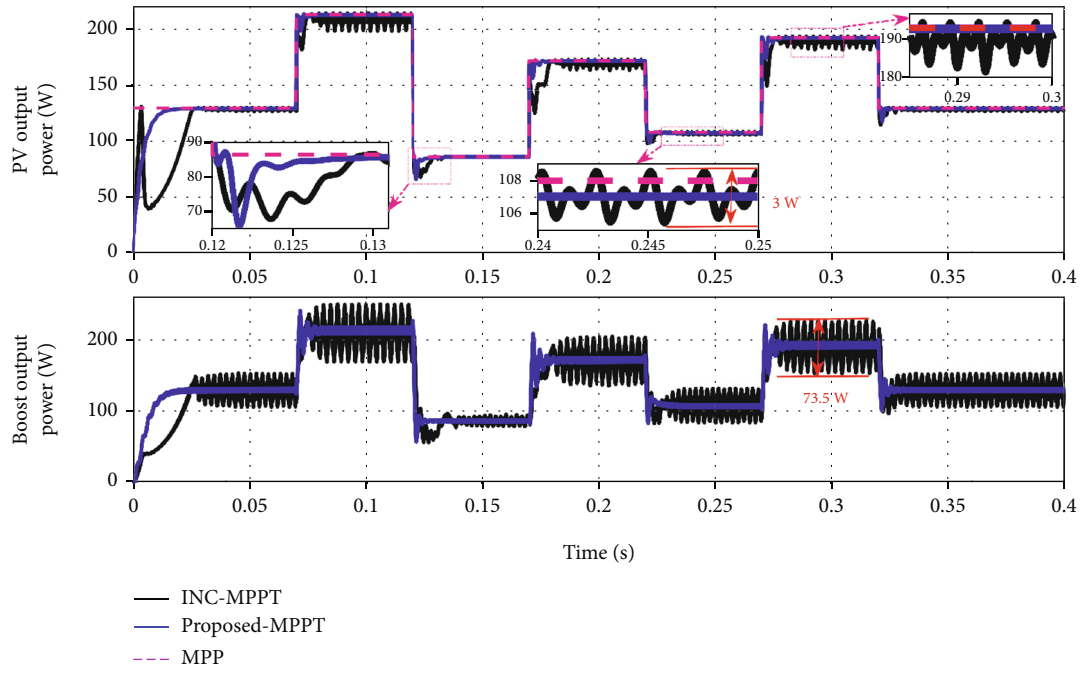

Figure 12: Comparison of the simulation results of the output PV and boost converter power.

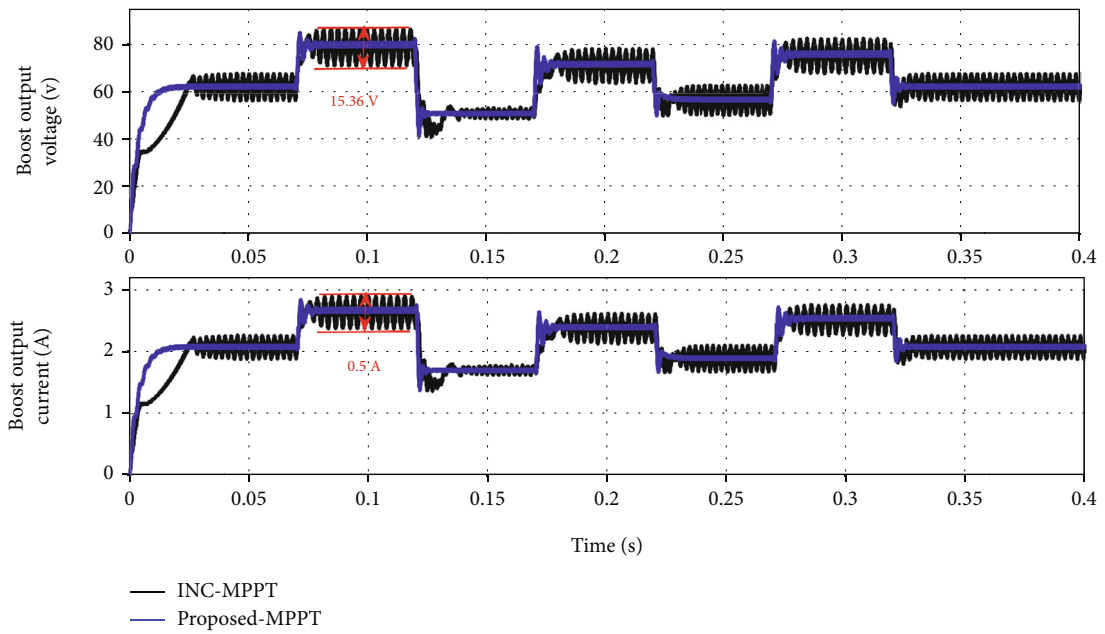

Figure 13: Comparison of the simulation results of the output voltage and current of the boost converter.

zero steady-state ripples around the MPP. Moreover, the proposed MPPT scheme is able to eliminate the large ripple magnitude obtained in the case of using the INC MPPT scheme and to provide good stability in the output power, current, and voltage of the boost converter, as depicted in Figures 8 and 9. This good stability can greatly minimize the stress of the electronic components.

In addition to the aforementioned performances, the proposed MPPT scheme can enhance the tracking efficiency by 5.63% compared to the INC MPPT scheme as shown in Figure 10. Moreover, it shows great ripple mitigation in the output boost converter power, current, and voltage compared to the INC MPPT scheme, as reported in Table 2. According to the latter, the reduction in ripple in output

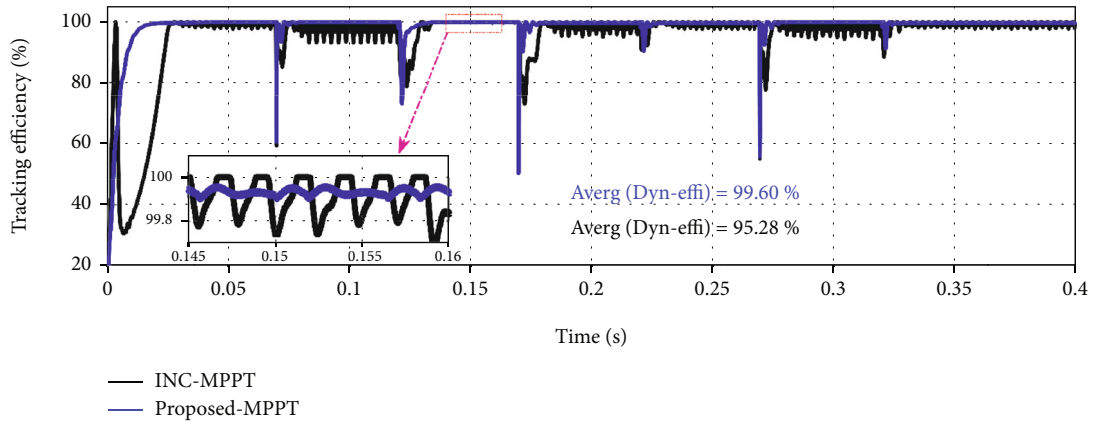

Figure 14: Dynamic efficiency tracking of the simulation results.

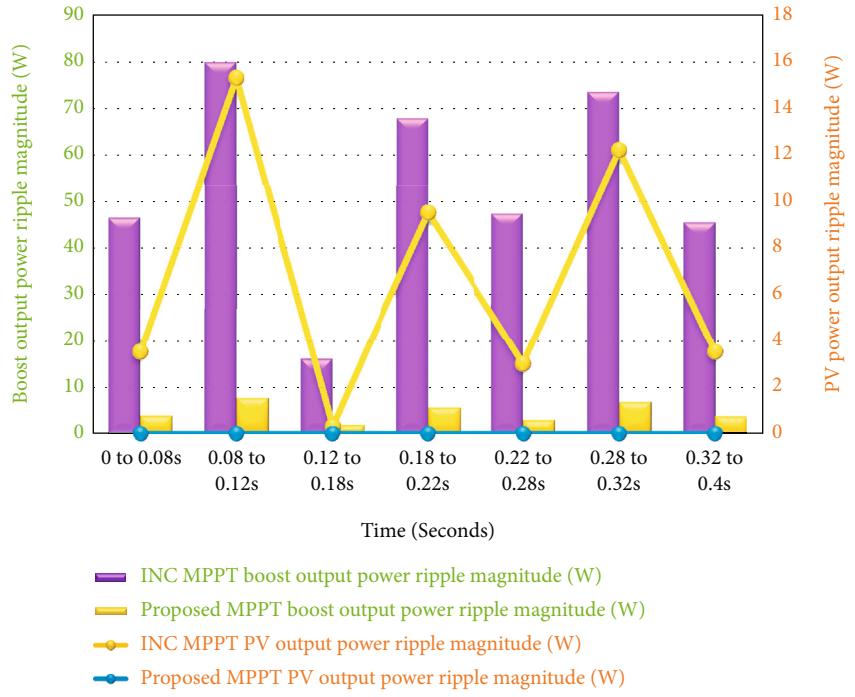

Figure 15: Photovoltaic and boost converter output power ripple magnitude of INC and proposed MPPT schemes.

power, current, and voltage using the suggested MPPT scheme instead of the INC MPPT scheme is 32.1%, 16.26%, and 16.8%, respectively.

The ripple magnitude (h) in an output signal can be calculated as follows [38]:

$$h = h_1 - h_2, \tag{9}$$

where h_1 and h_2 are the upper and lower bounds of the ripple in the output signal.

The steady-state error (SSE) of photovoltaic power can be calculated as follows [38]:

$$\mathrm{SSE} = P_{\mathrm{MPP}} - \left[h_2 + \frac{h_1 - h_2}{2}\right], \tag{10}$$

where P_{MPP} is the photovoltaic power at MPP.

4.2. Rapid Irradiance Change Scenario Analysis Results. The rapid solar irradiation scenario shown in Figure 11 is carried out to examine the tracking ability and the speed

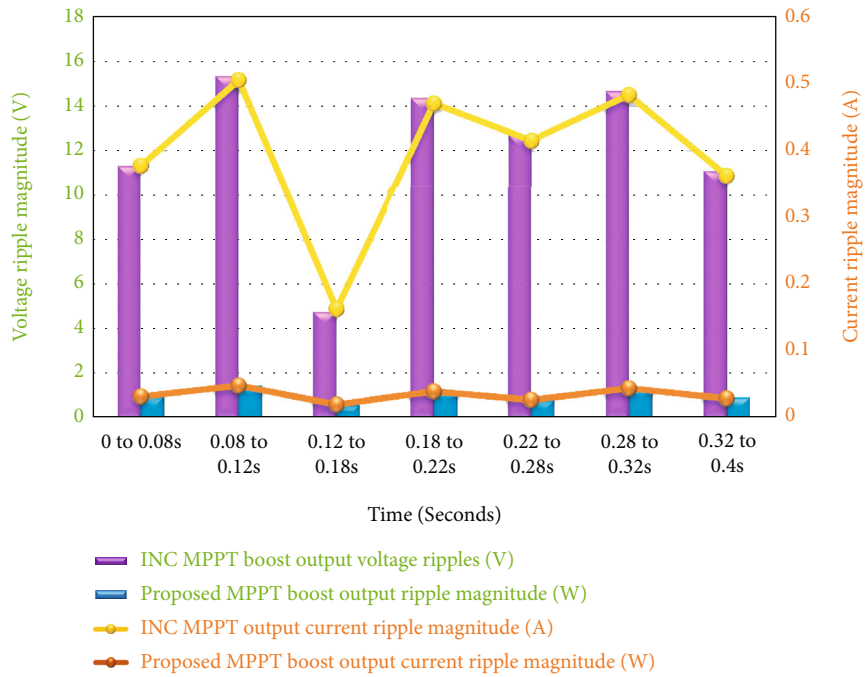

Figure 16: Output current and voltage ripple magnitude of the boost converter using INC and the proposed MPPT schemes.

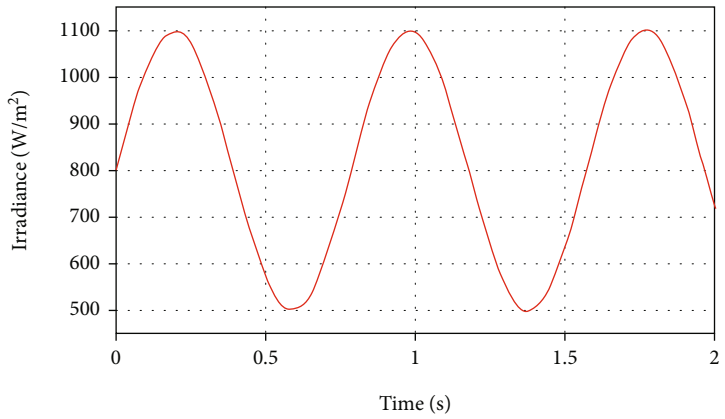

Figure 17: Sin irradiance profile.

convergence of the suggested MPPT scheme to track the MPP under an abrupt sun irradiation change.

Figures 12 and 13 show the simulation results of both MPPT schemes. It should be noted that the suggested MPPT scheme shows good tracking of the MPP during the whole scenario, and according to Figure 12, it is noticeable that the PV power curve is close to the MPP curve. Moreover, the proposed MPPT scheme can greatly reduce the ripple magnitude of the boost converter output current and voltage compared to the INC MPPT scheme, which shows large fluctuations in the output current and voltage that lead to nonstability of the system. Besides, the INC MPPT scheme has a slow time response, as depicted in Figure 12. On the contrary, the suggested MPPT scheme can obviously enhance the convergence time under all conditions of sudden irradiance change.

The curves obtained for the dynamic tracking efficiency under sudden insolation change of both MPPT schemes are presented in Figure 14. In this context, as can be seen from Figure 14, the suggested MPPT scheme shows the best dynamic tracking efficiency with an average of 99.60%. In contrast, the INC MPPT scheme shows a moderate dynamic tracking efficiency, which can drop down to 88%, especially at the sudden change of insolation, with its average tracking efficiency of about 95.28%.

A detailed comparison of the performance of the suggested MPPT scheme over the INC MPPT scheme in the cases of the reduction of ripple magnitude in photovoltaic and boost converter output power, current, and voltage is depicted in Figures 15 and 16. As can be seen, the proposed MPPT scheme greatly reduces the ripple magnitude compared to the INC approach, leading to high stability of the overall system.

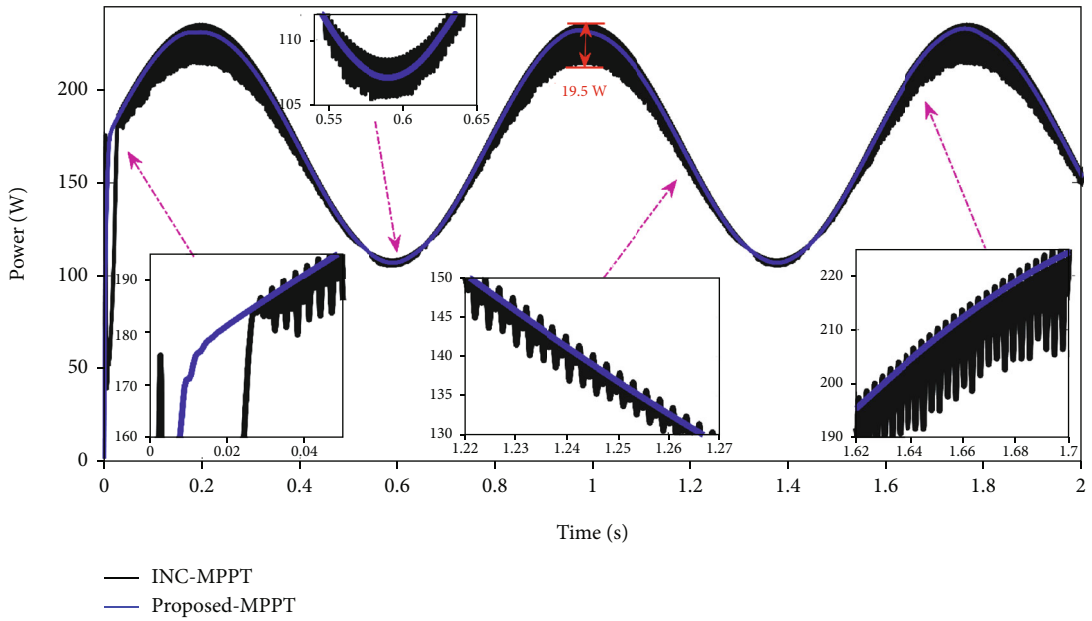

Figure 18: Photovoltaic output power curves of INC and the proposed MPPT schemes.

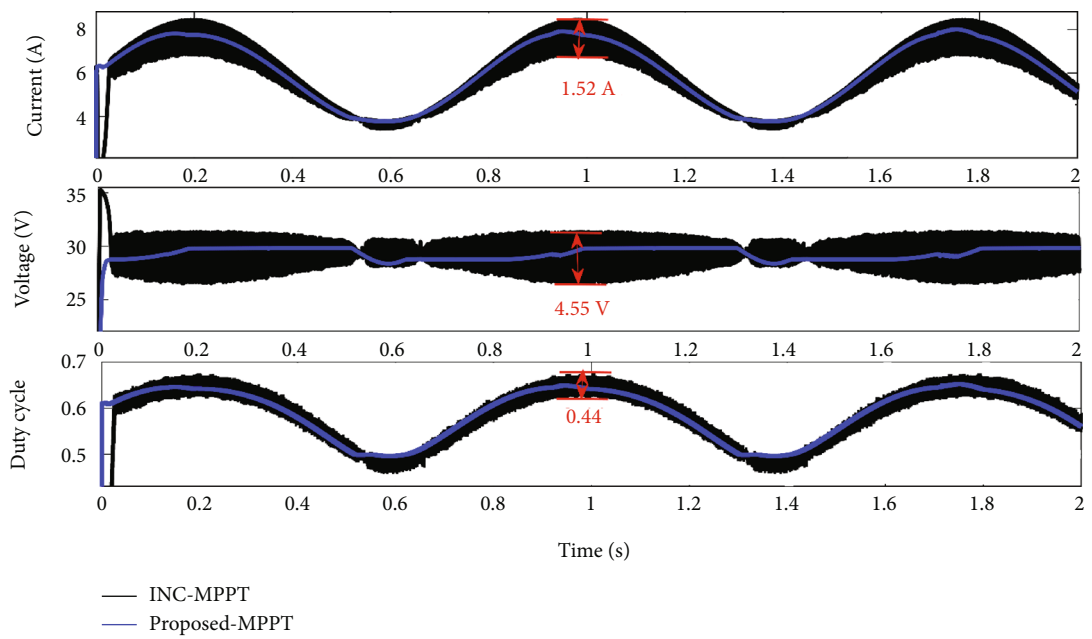

Figure 19: Photovoltaic output voltage and current with duty cycle of the boost converter curves.

4.3. Sin Irradiance Change Scenario Analysis Results. In order to show the dynamic behavior of the suggested MPPT scheme and to assess its robustness and performance, a Sin form of sun irradiation change scenario is suggested, where the insolation levels ranged from 0.5 kW/m^2 to 1.1 kW/m^2 as shown in Figure 17, while the temperature was fixed at 25° C.

Figure 18 illustrates the curves extracted from the output power of the photovoltaic module using both MPPT schemes. It is obvious that the suggested scheme tracks the available MPP of the photovoltaic module by immediately following the solar irradiation variation profile. Indeed, it can extract the real MPP with zero oscillations and better performance, as illustrated in the zoomed-in views of Figure 18 and it provides faster time converging to the MPP. On the contrary, despite following the insolation variation profile, the INC MPPT scheme shows a slow time response and high oscillation amplitude around the MPP, especially for high irradiance levels, leading to significant power losses.

Furthermore, the photovoltaic output current and voltage with duty cycle waveform simulation results are depicted in Figure 19, while the boost converter output power, current, and voltage simulation results are shown in Figure 20

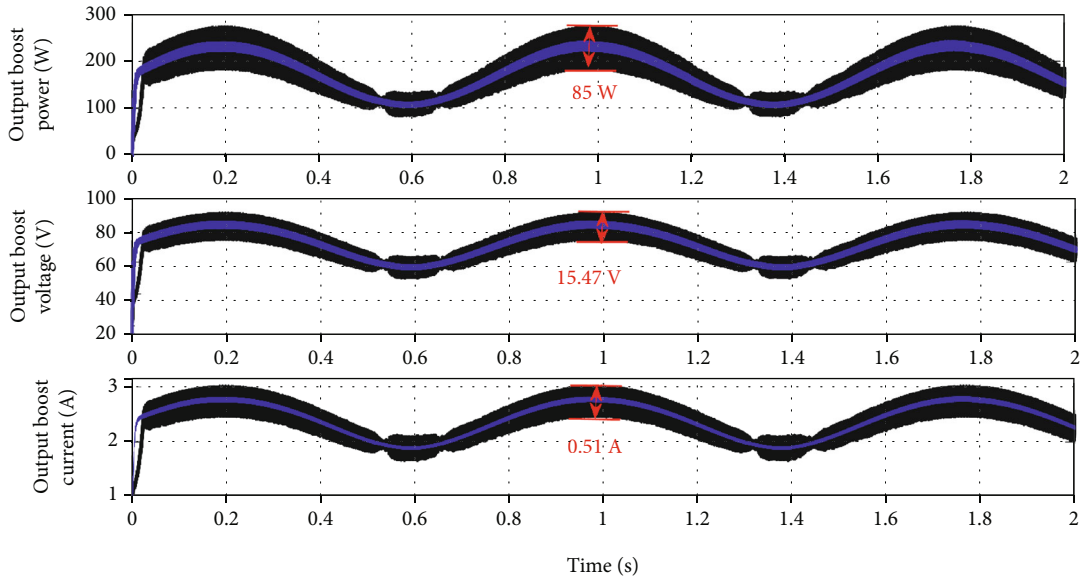

Figure 20: Output power current and voltage of the boost converter.

Table 3: Summary of the simulation results comparison of INC and the proposed MPPT schemes under the Sin scenario.

Sin test	INC MPPT	Proposed MPPT
Average tracking efficiency (%)	97.87	99.62
Time response (seconds)	0.028	0.012
Average ripple magnitude of the boost output current (A)	1.85	0.08
Average ripple magnitude of the boost output voltage (V)	14.38	2
Average ripple magnitude of the boost output power (W)	54.52	10.62
Average ripple magnitude of the photovoltaic voltage (V)	3.5	Neglected
Average ripple magnitude of the photovoltaic current (A)	0.35	Neglected
Average ripple magnitude of the photovoltaic power (A)	10.8	Neglected

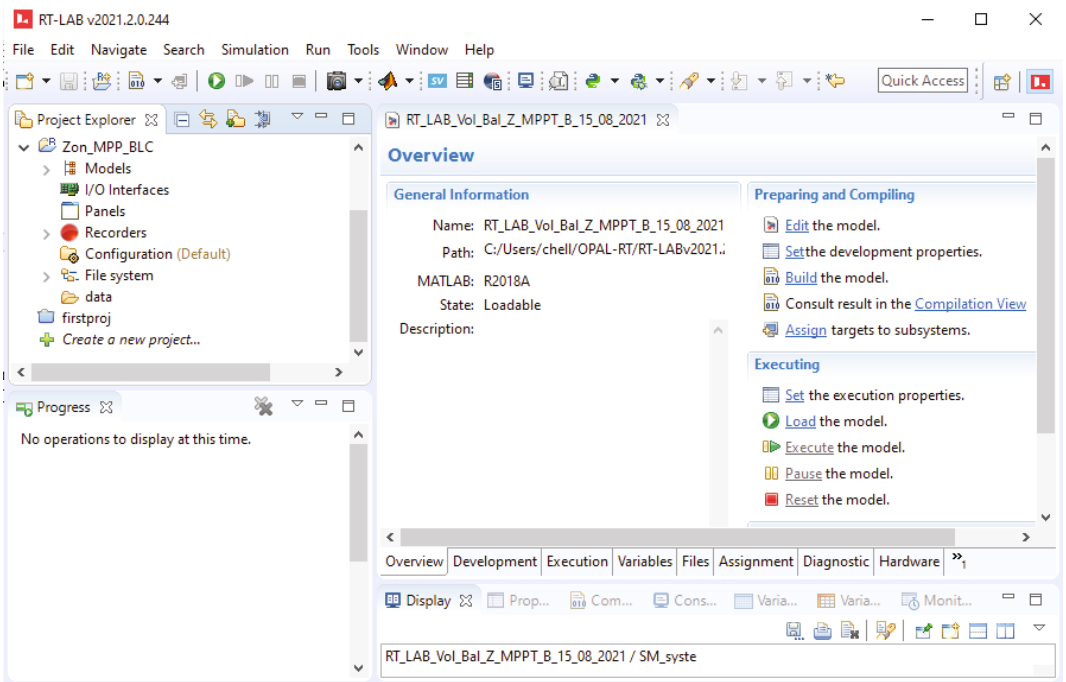

Figure 21: RT-LAB platform.

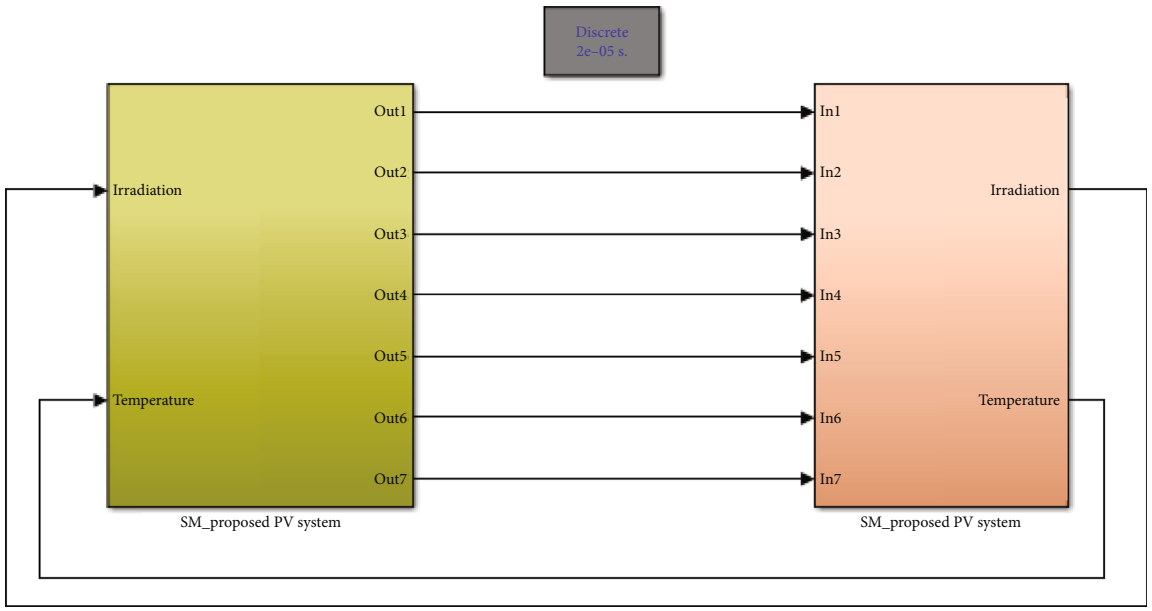

Figure 22: Simulink schematic modeling-based RT-LAB simulator of the complete PV system.

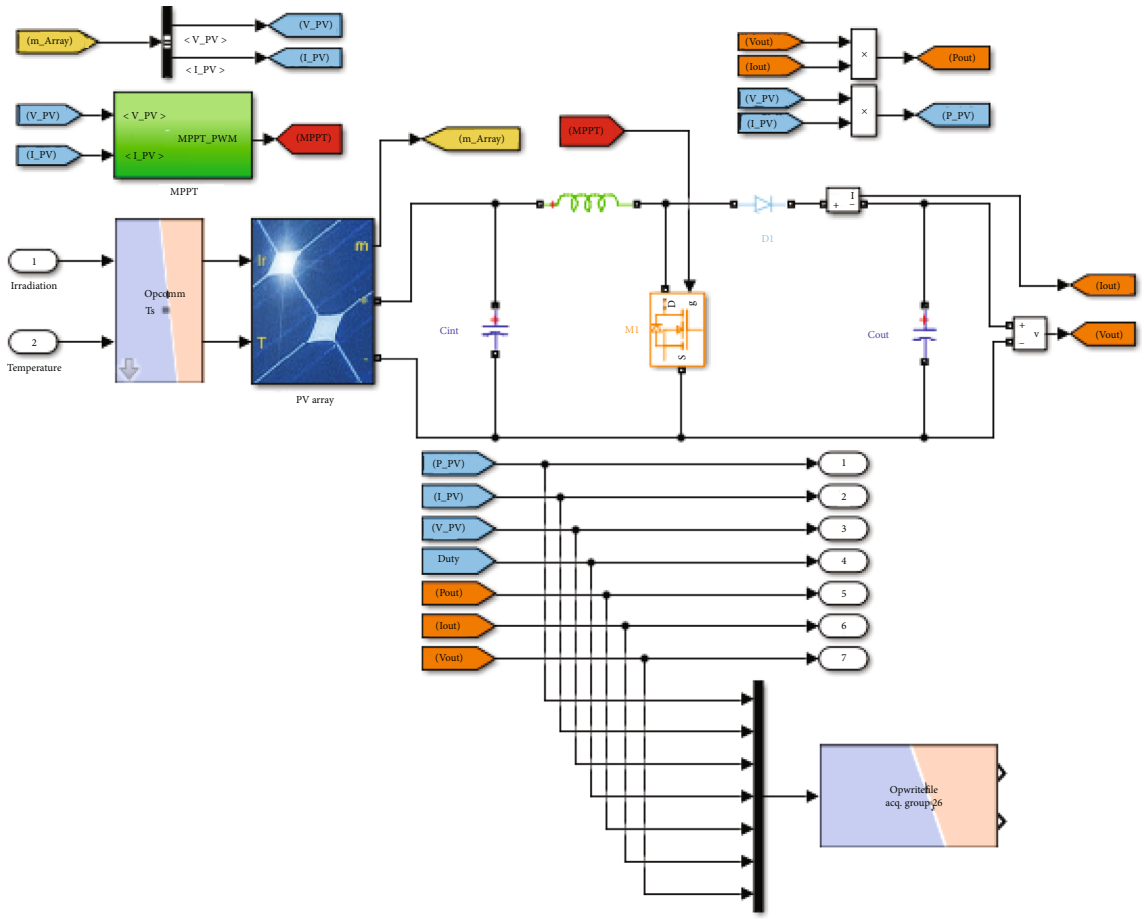

Figure 23: Contents of the SM subsystem diagram.

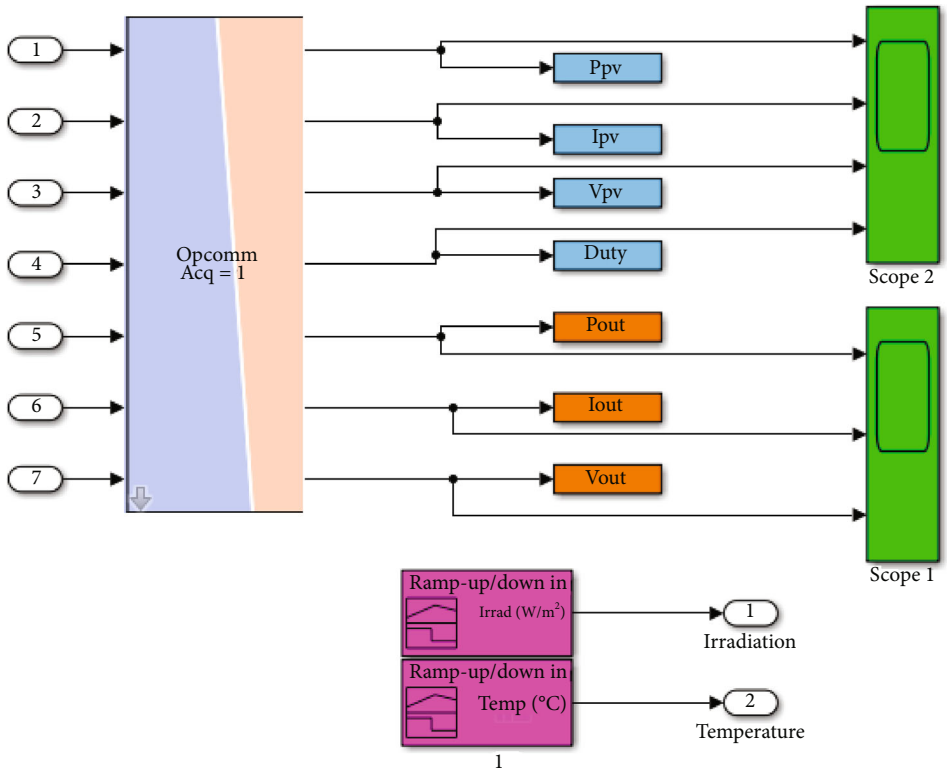

Figure 24: Contents of the SC subsystem diagram before the compilation of RT-LAB.

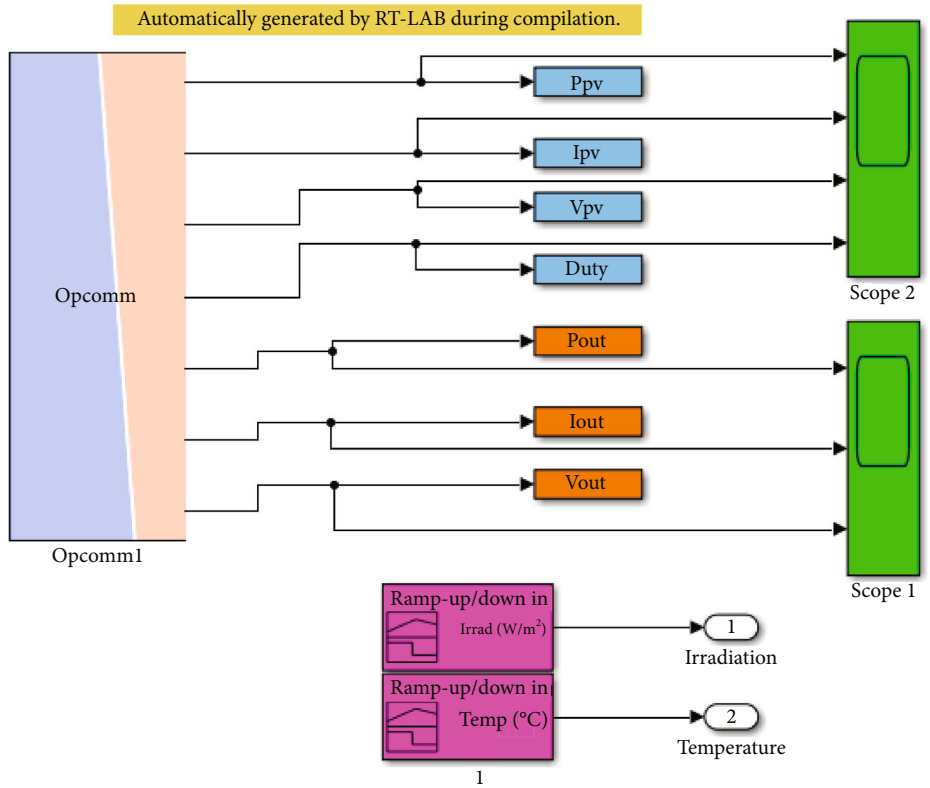

Figure 25: Contents of the SC subsystem diagram after the compilation of RT-LAB.

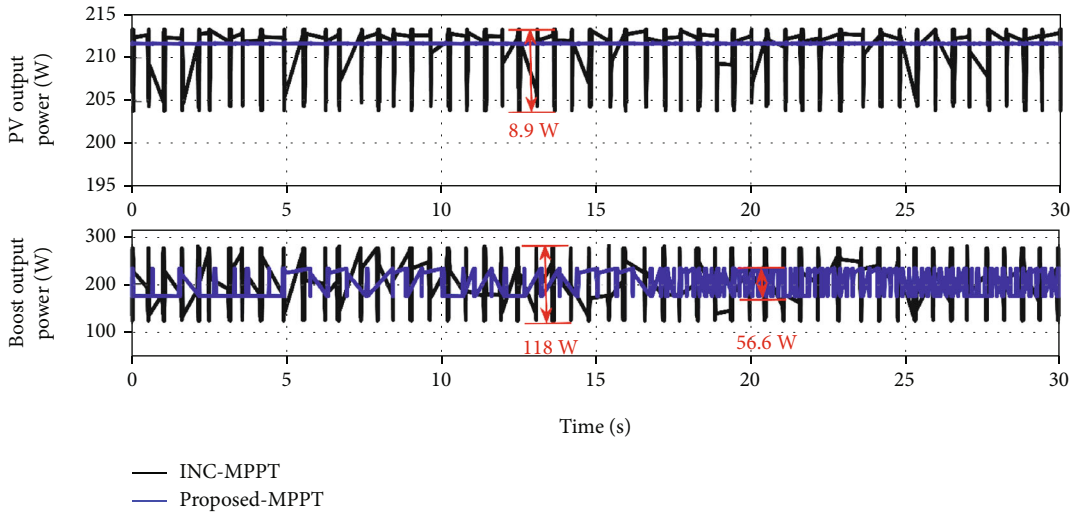

Figure 26: RT-LAB real-time results of the PV array and TLBC power waveforms of both MPPT schemes under STC.

for both MPPT schemes. On the basis of these figures, it can be seen that the proposed MPPT scheme significantly minimizes the ripple magnitude on the output side of the boost converter and provides good stability for the whole system. On the other hand, high ripple magnitude with nonstability is observed in the power, current, and voltage of the output boost converter side in the case of using the INC MPPT scheme.

Table 3 shows the summary of the simulation results comparison of the INC method and the proposed MPPT scheme during the Sin scenario. In light of this comparison, it is worth mentioning that the proposed MPPT scheme can considerably enhance the overall efficiency of the photovoltaic system and reduce the loss of power energy.

5. Real-Time Verification Using the RT-LAB Simulator Environment

RT-LAB (Real-Time-Laboratory) [39] is a software environment of the OPAL-RT simulation system, as shown in Figure 21. It is fully integrated with MATLAB software and compatible to work with fixed-step solvers in the Simulink environment. Furthermore, it has been considered one of the most adequate and relevant real-time simulators used to date to perform and evaluate many power system engineering applications, such as renewable energy, robotics, aerospace, and automotive applications [40–42]. Furthermore, the application of the RT-LAB platform in renewable energy, especially solar photovoltaic systems, has gained more consideration and has become an interesting tool to be used in the implementation and examination of the control performance of the entire photovoltaic system, for example, the MPPT controller [41, 43, 44].

Figure 22 presents the Simulink schematic modeling-based RT-LAB simulator of the complete photovoltaic system, which consists of two main subsystems: SM (Master Subsystem) and SC (Console Subsystem). The SM subsystem's role is summarized in the real-time calculation and data synchronization, whereas the SC subsystem's role is considered as the unique user interface to interact with the system during execution [42]. To get synchronization communication between the two SM and SC subsystems, the OpComm block depicted in Figures 23 and 24 should be used. The contents of the SM block with the SC block contents before and after RT-LAB compilation are shown in Figures 23, 24, and 25, respectively.

To validate the results obtained using the simulation in the previous section, real-time validation was carried out using the RL-LAB simulator, in which the accuracy and performance of the novel MPPT scheme were compared with the INC scheme under different weather conditions.

5.1. Results of Standard Test Conditions (TSC) Analysis. Figures 26, 27, and 28 illustrate the results obtained during the STC (1 kW/m^2, 25°C). Figures 26 and 27 depict the waveforms of the PV module and boost converter output power, current, and voltage in addition to the duty ratio generated by both MPPT schemes. Furthermore, the tracking efficiency is presented in Figure 28.

With regard to these results, it is clear that the real-time implementation of the two MPPT schemes using the RL-LAB environment was executed accurately. Certainly, the INC scheme can track the MPP, but bulky fluctuations and obvious disturbances in the output waveforms of the photovoltaic module and DC-DC boost converter are manifest. Consequently, a mediocre average tracking efficiency of 97.80% is achieved, as shown in Figure 28. In contrast, when using the novel MPPT scheme, the aimed MPP is tracked perfectly without oscillations, and the average tracking efficiency can reach 99.80%. Furthermore, good stability of the output current and voltage of the photovoltaic module with significant reduction in output ripple magnitude of the current, voltage, and power of the DC-DC boost converter is obtained.

5.2. Results of Sudden Irradiance Change Analysis. To examine and assess the performance of the novel MPPT scheme, another test was carried out under sudden solar irradiation

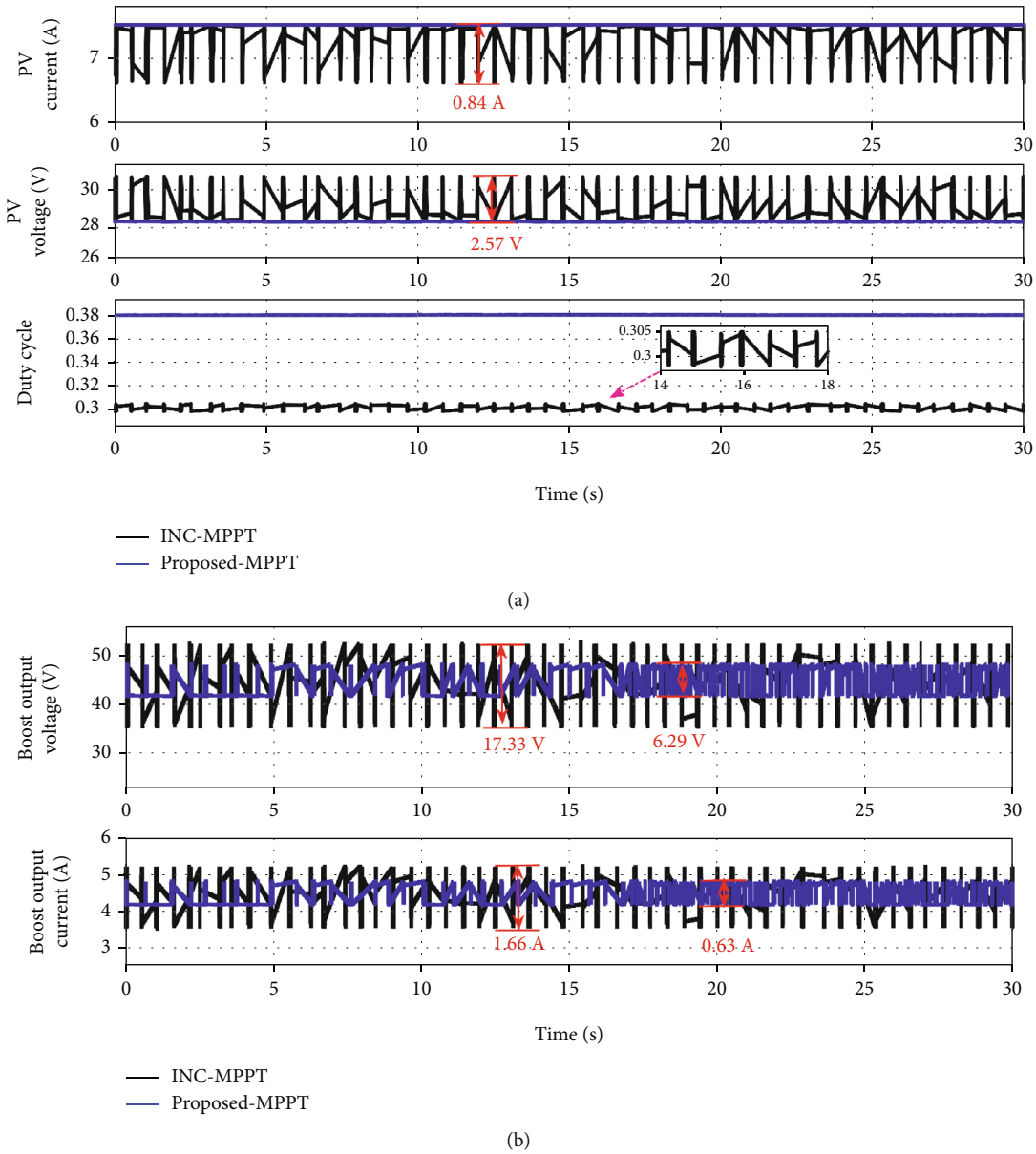

Figure 27: RT-LAB real-time results of the output current and voltage waveforms of both MPPT schemes under STC: (a) PV array and (b) TLBC.

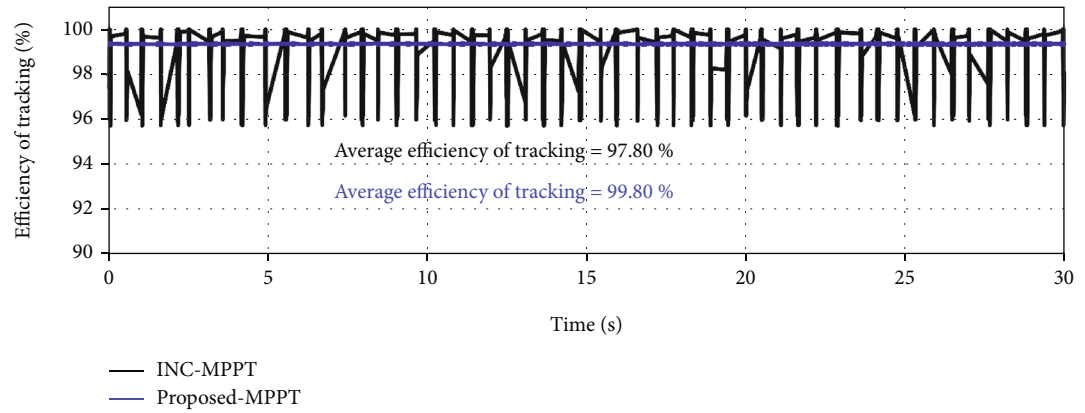

Figure 28: RT-LAB real-time results of the tracking efficiency comparison waveforms of both MPPT schemes under STC.

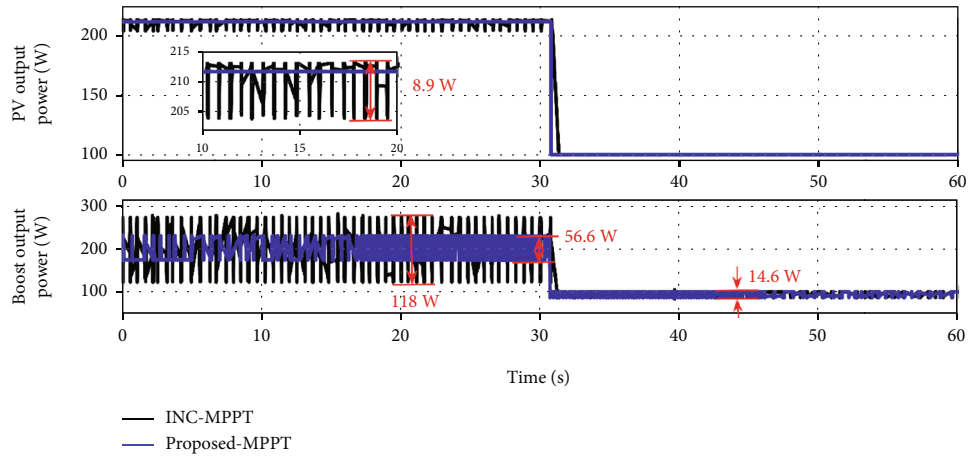

Figure 29: RT-LAB real-time results of the PV array and TLBC output power waveforms of both MPPT schemes under the sudden change of insolation.

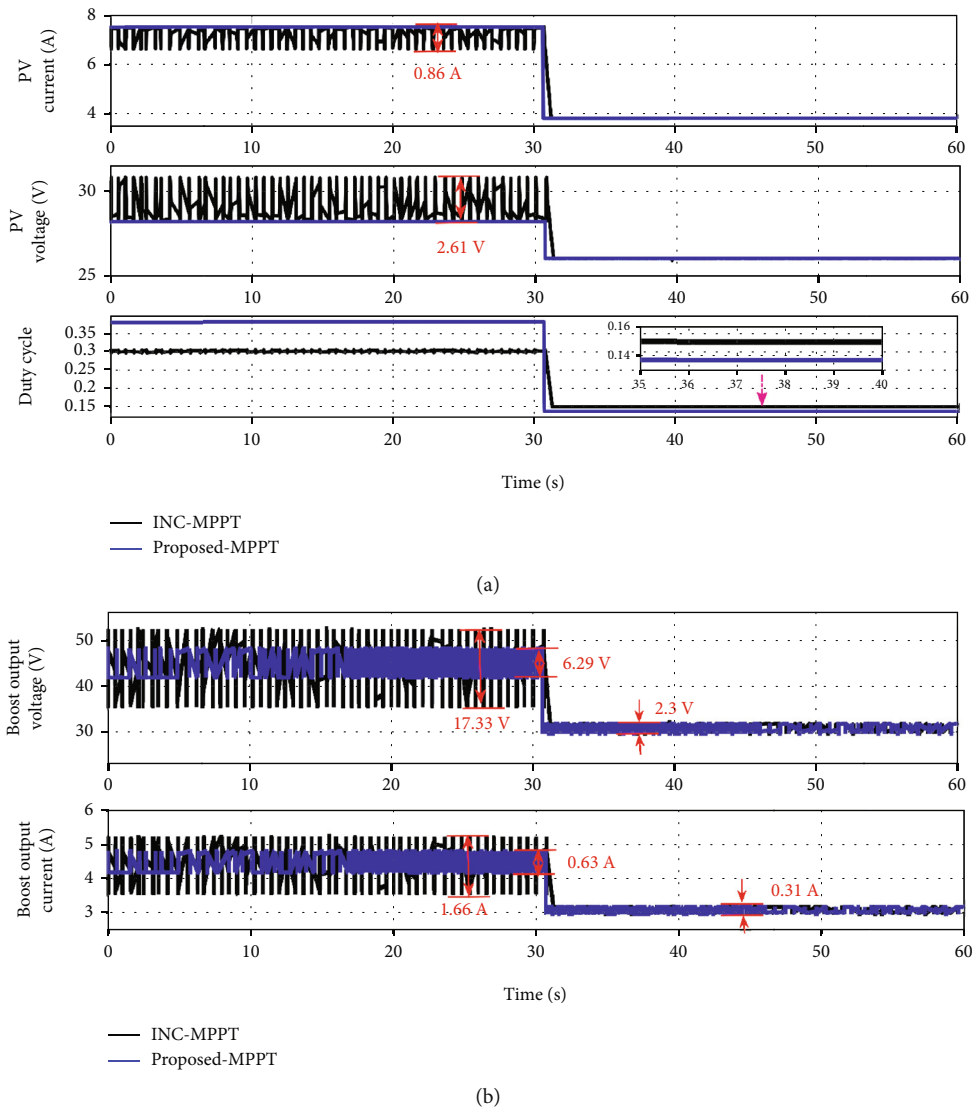

Figure 30: RT-LAB real-time results of both MPPT schemes under the sudden insolation change: (a) PV array output current and voltage with duty ratio curves and (b) boost converter output current and voltage waveforms.

Table 4: Summary of the performance comparison of the proposed MPPT and INC MPPT schemes during real-time verification using the RT-LAB simulator.

Test conditions	INC MPPT		Proposed MPPT	
	STC	Sudden insolation change ($1 \rightarrow 0.5\,kW/m^2$)	STC	Sudden insolation change ($1 \rightarrow 0.5\,kW/m^2$)
Average tracking efficiency (%)	97.80	96.5	99.80	97.77
Ripple magnitude of the boost converter output current (A)	1.66	1.66-0.31	0.63	0.63-0.31
Ripple of magnitude of the boost converter output voltage (V)	17.33	17.33-2.3	6.29	6.29-2.3
Average ripple of magnitude of the boost converter output power (W)	118	118-14.9	56.6	56.6-14.9
Average ripple magnitude of the photovoltaic voltage (V)	2.61	2.61-neglected	Neglected	Neglected
Average ripple magnitude of the photovoltaic current (A)	0.86	0.86-neglected	Neglected	Neglected
Average ripple magnitude of the photovoltaic power (A)	8.8	8.9-neglected	Neglected	Neglected

Table 5: Performance comparison of the proposed MPPT scheme with other MPPT schemes.

Scenario	Ref [31]	Ref [34]	Ref [30]	INC method	Proposed
Steady-state oscillation	Small	Small	Neglected	Big	Neglected
Static tracking efficiency (%)	99.70	95.43	99.52	94.23	99.86
Tracking time (s)	0.12	0.08	0.016	0.028	0.011
Dynamic tracking efficiency (%)	96.61	98.95	99.68	95.28	99.60
Tracking velocity under fast change in irradiance	Medium	Medium	Fast	Medium	Very fast

variation, where the insolation varies abruptly from $1\,kW/m^2$ to $0.5\,kW/m^2$ in a real-time simulation process. The results obtained throughout these test conditions are described in Figures 29 and 30.

According to the dynamic response curves of the PV module output power depicted in Figure 29, it is notable that the proposed MPPT scheme successfully tracks the expected MPP without fluctuation during the overall test time. In addition, it offers a fast tracking speed reaction under the sudden change in solar irradiation, unlike the INC scheme, which shows a slow tracking reaction under the rapid irradiance change; in the same fashion, huge oscillations manifest around the MPP at a high level of insolation ($1\,kW/m^2$). Additionally, the output power, current, and voltage of the DC-DC boost converter suffer from a large ripple magnitude with noticeable instability when the INC scheme is used as revealed in Figure 30. On the contrary, when using the proposed scheme, minimized ripples with good stability appear in the output power, current, and voltage of the DC-DC boost converter. This is due to the adequate generated duty ratio by the proposed scheme, as revealed in Figure 30(a).

Table 4 shows the summary of the average performance of the proposed MPPT scheme compared to the INC MPPT scheme under real-time verification using the RT-LAB simulator. Here, the average tracking efficiency, the output ripple magnitude of the DC-DC boost converter, and the photovoltaic array are considered in the performance comparison. This comparison shows that the proposed MPPT scheme outperforms the INC MPPT scheme in terms of providing high tracking efficiency and minimizing the DC-DC boost converter and PV array output ripple amplitude. In this context, the proposed MPPT scheme has the highest tracking efficiency with the lowest output ripple magnitude from the DC-DC boost converter and the PV array, respectively.

5.3. Performance Evaluation. The performance analysis of the proposed MPPT scheme compared to previously published MPPT techniques is reported in Table 5. In light of this comparison, it is worth mentioning that the proposed scheme can noticeably improve the tracking performance compared to other techniques in the cases of static and dynamic tracking efficiency, tracking time, and steady-state fluctuation. Indeed, the proposed MPPT scheme provides the highest tracking efficiency and velocity with the lowest tracking time compared to other published MPPT techniques.

6. Conclusion

In this paper, a novel MPPT scheme is used to enhance the tracking performance of the photovoltaic system under varying solar irradiation. In addition, it is used to overcome the high ripple magnitude problem on the output side of the

boost converter, which most conventional MPPT schemes suffer from. The implementation of the suggested MPPT scheme with the whole photovoltaic system is carried out under two tools, namely, the MATLAB/Simulink® and RT-LAB simulator. The first tool is used to offer simulation verification, while the second tool is used to provide real-time verification. The performance and accuracy of the proposed MPPT scheme have been carried out through various tests with different solar irradiance scenarios and compared with those of the INC MPPT scheme. In light of the comparative results in both environments, it should be noted that the proposed MPPT scheme can obviously enhance the tracking performance and overcome the ripple problem in the output of the boost converter. Indeed, it provides the fastest time response to locate the MPP and the best tracking efficiency under the overall scenarios, with an average tracking efficiency of 99.69% and 98.78% using the MATLAB/Simulink® and RT-LAB simulator tools, respectively, whereas the INC MPPT scheme can only have an average tracking efficiency of 95.79% and 97.15% using both tools, respectively. Future research work will focus on three main points: an experimental evaluation of the proposed MPPT approach's performance with the complete photovoltaic system, an improvement to its tracking performance for use in PSC, and an additional comparison of its performance with newly published MPPT techniques.

Nomenclature

ABC: Artificial bee colony
ACO: Ant colony optimization
FOCV: Fractional open-circuit voltage
FLC: Fuzzy logic control
FSCC: Fractional short-circuit current
GMPP: Global maximum power point
HC: Hill climbing
INC: Increment of conductance
LMPP: Local maximum power point
MPP: Maximum power point
MPPT: Maximum power point tracking
NNA: Neural network algorithm
OP: Operating point
P&O: Perturb and observe
PSC: Partial shading conditions
PSO: Particle swarm optimization
STC: Standard test conditions
RT-LAB: Real-Time-Laboratory
I-P: Current versus power characteristics of the photovoltaic module
P-V: Power versus voltage characteristics of the photovoltaic module
I_{pv}: Photovoltaic cell output current [A]
I_{ph}: Current of photovoltaic cell [A]
N_P, N_S: Numbers of solar power cells in parallel and in series
Q: Electronic charge value $[1.6 \times 10^{-19}\text{C}]$
V_{pv}: Photovoltaic cell output voltage [V]
A: Dimensionless junction material factor
k: Boltzmann's constant $[8.65 \times 10^{-5} eV/K]$
T: Temperature of the p-n junction [K]
k_i: Short-circuit current temperature coefficient [%/°C]
T_r: Cell reference temperature [°C]
G: Solar irradiation [W/m^2]
I_s: Saturation current [A]
R_{out}: Boost converter output resistance [Ω]
R_{load}: Load resistance at instant (t) [Ω]
$d(k)$: Duty cycle of the boost converter at instant (k)
dI_{pv}: Change in photovoltaic current [W]
dV_{pv}: Change in photovoltaic voltage [W]
dP_{pv}: Change in the photovoltaic power [W]
$C_{\text{in}}, C_{\text{out}}$: Input and output capacitor of the boost converter [F]
P_{pv}: Photovoltaic output power [W]
V_t: PV cell thermal voltage (V).

Data Availability

The authors can confirm that all relevant data are included in the article and no supplementary information files are available.

Conflicts of Interest

All authors have declared no competing of interests.

References

[1] IRENA, *Climate Change and Renewable Energy: National Policies and the Role of Communities, Cities and Regions (Report to the G20 Climate Sustainability Working Group (CSWG))*, International Renewable Energy Agency, Abu Dhabi, 2019.

[2] A. Chellakhi, S. El Beid, and Y. Abouelmahjoub, "Ripples Amplitude Minimizing of the Output Boost Converter Using An Innovative MPPT Controller for PV Systems Applications," in *2020 IEEE 2nd International Conference on Electronics, Control, Optimization and Computer Science (ICECOCS)*, pp. 1–6, Kenitra, Morocco, 2020.

[3] A. Chellakhi, S. El Beid, and Y. Abouelmahjoub, "An improved maximum power point approach for temperature variation in PV system applications," *International Journal of Photoenergy*, vol. 2021, Article ID 9973204, 21 pages, 2021.

[4] M. Mao, L. Cui, Q. Zhang, K. Guo, L. Zhou, and H. Huang, "Classification and summarization of solar photovoltaic MPPT techniques: a review based on traditional and intelligent control strategies," *Energy Reports*, vol. 6, pp. 1312–1327, 2020.

[5] A. M. Eltamaly and Y. A. Almoataz, *Modern Maximum Power Point Tracking Techniques for Photovoltaic Energy Systems*, Springer, 2020.

[6] C. H. Basha and C. Rani, "Different conventional and soft computing MPPT techniques for solar PV systems with high step-up boost converters: a comprehensive analysis," *Energies*, vol. 13, no. 2, p. 371, 2020.

[7] B. Yang, T. Zhu, J. Wang et al., "Comprehensive overview of maximum power point tracking algorithms of PV systems under partial shading condition," *Journal of Cleaner Production*, vol. 268, p. 121983, 2020.

[8] A. Chellakhi, S. El Beid, and Y. Abouelmahjoub, "Implementation of a novel MPPT tactic for PV system applications on MATLAB/Simulink and Proteus-based Arduino board environments," *International Journal of Photoenergy*, vol. 2021, Article ID 6657627, 19 pages, 2021.

[9] N. Kumar, B. Singh, B. K. Panigrahi, C. Chakraborty, H. M. Suryawanshi, and V. Verma, "Integration of solar PV with low-voltage weak grid system: using normalized Laplacian kernel adaptive Kalman filter and learning based InC algorithm," *IEEE Transactions on Power Electronics*, vol. 34, no. 11, pp. 10746–10758, 2019.

[10] S. A. Rizzo and G. Scelba, "A hybrid global MPPT searching method for fast variable shading conditions," *Journal of Cleaner Production*, vol. 298, article 126775, 2021.

[11] N. Kumar, B. Singh, and B. K. Panigrahi, "Integration of solar PV with low-voltage weak grid system: using maximize-M Kalman filter and self-tuned P&O algorithm," *IEEE Transactions on Industrial Electronics*, vol. 66, no. 11, pp. 9013–9022, 2019.

[12] A. Chellakhi, B. S. El, Y. Abouelmahjoub, and Y. Mchaouar, "Optimization of power extracting from photovoltaic systems based on a novel adaptable step INC MPPT approach," *IFAC-PapersOnLine*, vol. 55, no. 12, pp. 508–513, 2022.

[13] A. Chellakhi, S. El Beid, and Y. Abouelmahjoub, "An improved adaptable step-size P&O MPPT approach for stand-alone PV systems with battery station," 2021, https://ssrn.com/abstract=3869535.

[14] S. Bhattacharyya, P. D. S. Kumar, S. Samanta, and S. Mishra, "Steady output and fast tracking MPPT (SOFT-MPPT) for P&O and InC algorithms," *IEEE Transactions on Sustainable Energy*, vol. 12, no. 1, pp. 293–302, 2021.

[15] H. Abouadane, A. Fakkar, D. Sera, A. Lashab, S. Spataru, and T. Kerekes, "Multiple-power-sample based P&O MPPT for fast-changing irradiance conditions for a simple implementation," *IEEE Journal of Photovoltaics*, vol. 10, no. 5, pp. 1481–1488, 2020.

[16] N. Kumar, B. Singh, B. K. Panigrahi, and L. Xu, "Leaky-least-logarithmic-absolute-difference-based control algorithm and learning-based InC MPPT technique for grid-integrated PV system," *IEEE Transactions on Industrial Electronics*, vol. 66, no. 11, pp. 9003–9012, 2019.

[17] A. Nadeem, H. A. Sher, and A. F. Murtaza, "Online fractional open-circuit voltage maximum output power algorithm for photovoltaic modules," *IET Renewable Power Generation*, vol. 14, no. 2, pp. 188–198, 2020.

[18] S. Motahhir, A. El Hammoumi, and A. El Ghzizal, "The most used MPPT algorithms: review and the suitable low-cost embedded board for each algorithm," *Journal of Cleaner Production*, vol. 246, p. 118983, 2020.

[19] T. Zhu, J. Dong, X. Li, and S. Ding, "A comprehensive study on maximum power point tracking techniques based on fuzzy logic control for solar photovoltaic systems," *Frontiers in Energy Research*, vol. 9, 2021.

[20] M. N. Ali, K. Mahmoud, M. Lehtonen, and M. M. F. Darwish, "Promising mppt methods combining metaheuristic, fuzzy-logic and ann techniques for grid-connected photovoltaic," *Sensors (Switzerland)*, vol. 21, no. 4, p. 1244, 2021.

[21] A. M. Eltamaly, M. S. Al-Saud, A. G. Abokhalil, and H. M. H. Farh, "Simulation and experimental validation of fast adaptive particle swarm optimization strategy for photovoltaic global peak tracker under dynamic partial shading," *Renewable and Sustainable Energy Reviews*, vol. 124, p. 109719, 2020.

[22] N. Priyadarshi, S. Padmanaban, P. Kiran Maroti, and A. Sharma, "An extensive practical investigation of FPSO-based MPPT for grid integrated PV system under variable operating conditions with anti-islanding protection," *IEEE Systems Journal*, vol. 13, no. 2, pp. 1861–1871, 2019.

[23] S. Farajdadian and S. M. H. Hosseini, "Design of an optimal fuzzy controller to obtain maximum power in solar power generation system," *Solar Energy*, vol. 182, pp. 161–178, 2019.

[24] B. Babes, A. Boutaghane, and N. Hamouda, "A novel nature-inspired maximum power point tracking (MPPT) controller based on ACO-ANN algorithm for photovoltaic (PV) system fed arc welding machines," *Neural Comput & Applic*, vol. 34, no. 1, pp. 299–317, 2022.

[25] N. Priyadarshi, S. Padmanaban, L. Mihet-Popa, F. Blaabjerg, and F. Azam, "Maximum power point tracking for brushless DC motor-driven photovoltaic pumping systems using a hybrid ANFIS-FLOWER pollination optimization algorithm," *Energies*, vol. 11, no. 5, p. 1067, 2018.

[26] S. Padmanaban, N. Priyadarshi, M. S. Bhaskar, J. B. Holm-Nielsen, V. K. Ramachandaramurthy, and E. Hossain, "A hybrid ANFIS-ABC based MPPT controller for PV system with anti-islanding grid protection: experimental realization," *IEEE Access*, vol. 7, pp. 103377–103389, 2019.

[27] M. Premkumar, U. Subramaniam, T. Sudhakar Babu, R. M. Elavarasan, and L. Mihet-Popa, "Evaluation of mathematical model to characterize the performance of conventional and hybrid PV array topologies under static and dynamic shading patterns," *Energies*, vol. 13, no. 12, article 3216, 2020.

[28] L. G. K. Chai, L. Gopal, F. H. Juwono, C. W. R. Chiong, H. C. Ling, and T. A. Basuki, "A novel global MPPT technique using improved PS-FW algorithm for PV system under partial shading conditions," *Energy Conversion and Management*, vol. 246, article 114639, 2021.

[29] A. Ostadrahimi and Y. Mahmoud, "Novel spline-MPPT technique for photovoltaic systems under uniform irradiance and partial shading conditions," *IEEE Transactions on Sustainable Energy*, vol. 12, no. 1, pp. 524–532, 2021.

[30] A. Chellakhi, B. S. El, and Y. Abouelmahjoub, "A novel theta MPPT approach based on adjustable step size for photovoltaic system applications under various atmospheric conditions," *Energy Systems*, pp. 1–26, 2022.

[31] M. Premkumar and R. Sowmya, "An effective maximum power point tracker for partially shaded solar photovoltaic systems," *Energy Reports*, vol. 5, pp. 1445–1462, 2019.

[32] M. Premkumar, C. Kumar, R. Sowmya, and J. Pradeep, "A novel salp swarm assisted hybrid maximum power point tracking algorithm for the solar photovoltaic power generation systems," *Automatika*, vol. 62, no. 1, pp. 1–20, 2021.

[33] A. Chellakhi, S. El Beid, and Y. Abouelmahjoub, "An innovative fast-converging speed MPPT approach without oscillation for temperature varying in photovoltaic systems applications," *Energy Sources, Part A: Recovery, Utilization, and Environmental Effects*, vol. 44, no. 2, pp. 2674–2696, 2022.

[34] B. Babes, F. Albalawi, N. Hamouda, S. Kahla, and S. S. M. Ghoneim, "Fractional-Fuzzy PID Control approach of photovoltaic-wire feeder system (PV-WFS): simulation and HIL-based experimental investigation," *IEEE Access*, vol. 9, pp. 159933–159954, 2021.

[35] D. Emara, M. Ezzat, A. Y. Abdelaziz, K. Mahmoud, M. Lehtonen, and M. M. F. Darwish, "Novel control strategy for enhancing microgrid operation connected to photovoltaic

generation and energy storage systems," *Electronics*, vol. 10, no. 11, p. 1261, 2021.

[36] N. Karami, N. Moubayed, and R. Outbib, "General review and classification of different MPPT techniques," *Renewable and Sustainable Energy Reviews*, vol. 68, pp. 1–18, 2017.

[37] M. N. Ali, K. Mahmoud, M. Lehtonen, and M. M. F. Darwish, "An efficient fuzzy-logic based variable-step incremental conductance MPPT method for grid-connected PV systems," *IEEE Access*, vol. 9, pp. 26420–26430, 2021.

[38] R. Pradhan, *Development of new parameter extraction schemes and maximum power point controllers for photovoltaic power systems, [Ph.D. Thesis]*, 2014.

[39] RT-LAB software platformn.d., https://www.opal-rt.com/software-rt-lab-2-2/.

[40] S. S. Noureen, V. Roy, and S. B. Bayne, "An overall study of a real-time simulator and application of RT-LAB using MATLAB simpowersystems," in *2017 IEEE Green Energy and Smart Systems Conference (IGESSC)*, Long Beach, CA, USA, 2017- November.

[41] X. Yuan, Y. Zhao, and W. Zhu, "Real-time simulation and research on photovoltaic power system based on RT-LAB," *The Open Fuels & Energy Science Journal*, vol. 8, no. 1, pp. 183–188, 2015.

[42] S. Mikkili, A. K. Panda, and J. Prattipati, "Review of real-time simulator and the steps involved for implementation of a model from MATLAB/SIMULINK to real-time," *Journal of The Institution of Engineers (India): Series B*, vol. 96, no. 2, pp. 179–196, 2015.

[43] R. B. A. Koad, A. F. Zobaa, and A. El-Shahat, "A novel MPPT algorithm based on particle swarm optimization for photovoltaic systems," *IEEE Transactions on Sustainable Energy*, vol. 8, no. 2, pp. 468–476, 2017.

[44] V. R. Kolluru, K. Mahapatra, and B. Subudhi, "Real-time digital simulation and analysis of sliding mode and P&O MPPT algorithms for a PV system," *International Journal of Emerging Electric Power Systems*, vol. 16, no. 4, pp. 313–322, 2015.